# Appendix B

## Measuring the Strength of Slurry Phase Heterogeneous Catalysts

Hien N. Pham, John Reardon, and Abhaya K. Datye

Center for Microengineered Materials and Department of Chemical & Nuclear Engineering, University of New Mexico, Albuquerque, NM 87131

### Abstract

Fischer-Tropsch (F-T) synthesis is a process used to convert coal-derived syngas to hydrocarbon liquids and waxes. A slurry phase bubble-column reactor (SBCR) is the preferred reactor type due to improved heat and mass transfer and operational simplicity in terms of catalyst loading and discharge. A potential disadvantage in the SBCR versus a fixed-bed reactor is the attrition of the catalyst which can cause difficulty with the catalyst/wax separation, resulting in gradual loss of catalyst from the reactor. In this work, we have evaluated two approaches to measure the strength and attrition resistance of heterogeneous catalysts: uniaxial compaction and ultrasonic fragmentation. A commercial catalyst developed for F-T synthesis was tested along with a sample of an alumina support having a similar particle size distribution. It was found that the cumulative particle size mass distribution plots after ultrasonic fragmentation show significant differences in strength, whereas the same powders show small differences in strength as measured by the uniaxial compaction method. Erosion was found to be the dominant fragmentation mechanism for the alumina support whereas fracture was the dominant mechanism for the F-T catalyst. Ultrasonic fragmentation also was applied to Fe F-T catalysts containing a kaolin binder. The catalyst with the binder was very weak, comparable to the binderless catalyst. Further analysis using TEM showed that kaolin and the Fe F-T catalyst occurred as two distinct phases, with plate-like structures which did not help create strong interlocking forces between them. These results provide clues for the design of attrition resistant catalysts.

### Introduction

The Fischer-Tropsch synthesis (1) is a process to convert energy reserves of coal and natural gas into liquid transportation fuels. With dwindling supplies of crude oil, this process is expected to have increasing commercial importance. At present, F-T synthesis is being practiced in South Africa for converting coal-derived syngas ($CO + H_2$) into hydrocarbon waxes which are subsequently processed to the desired product slate. The U.S. Department of Energy is also supporting a program of catalyst development (1,2) and pilot plant testing (3) for indirect liquefaction of coal.

SASOL in South Africa first used a tubular fixed-bed reactor for F-T synthesis, where catalyst extrudates were packed in parallel tubes inside a single reactor (4). A fluidized bed reactor was then used because it had a much higher gas throughput than the fixed-bed reactor (4). However, SASOL found many potential advantages in carrying out the F-T reaction in a slurry phase based

on comparisons of all three systems. Hence, work was initially carried out on a small bench scale which later progressed to a pilot plant scale of the slurry reactor. The commercial slurry phase reactor achieved an availability of over 98% in its first year of operation in 1993, and the performance has been maintained ever since.

Currently, the SBCR is used to convert coal-derived syngas to waxy hydrocarbons via Fischer-Tropsch (F-T) synthesis (5,6). Syngas bubbles upwards through a slurry consisting of liquid wax and catalyst particles, diffuses into the slurry, and is converted into more wax by the F-T reaction. The advantages to using a SBCR are: it is simpler and cheaper to construct, it provides better heat transfer and temperature control inside the reactor to improve product yield and quality (7), and it allows the removal and addition of catalyst while the reactor is in operation, thereby improving the overall availability. A fixed-bed reactor for F-T synthesis leads to poor heat of reaction removal capability, nonuniform catalyst loading, low conversion efficiency, and bed plugging due to carbon laydown at high temperatures. Hence, a SBCR is more reliable for F-T synthesis (8).

A potential disadvantage in using a SBCR involves the attrition, or breaking-up, of catalysts. When a SBCR is used to produce lighter products, such as methanol, which are volatile, catalyst attrition may not affect reactor operation. However, attrition becomes a problem with the F-T process where heavy waxy products are being produced, and separation becomes difficult between the wax and smaller catalyst particles. Recent experience comes from the LaPorte plant, using a catalyst prepared by United Catalysts, Inc. (UCI), operated for the DOE by Air Products (3). In the LaPorte SBCR, the filter system was plugged after one day of operation, and there was difficulty with the external catalyst/wax separation resulting in gradual loss of catalyst from the reactor (3).

The requirements for catalyst agglomerates differ from those in other applications; for example, during postprocessing of ceramics, hard agglomerates may counteract compaction, decreasing the shrinkage rate of ceramic powders during sintering (9), hindering densification of ceramic parts, and generating flaws that reduce the strength of the sintered product (10), and degrade the uniformity of products such as paint. Hence, successful dispersion of powders often requires total elimination of agglomerates. On the other hand, agglomeration may be necessary, for example, for care of handling powders. In applications such as catalysts, excessive attrition of particles, for example, in a fluidized bed could have a strong negative impact on the overall economics of a plant. Unstable fluidization behavior and product contamination also could be caused by unexpectedly high attrition. Other examples include generation of very fine particles (dust) which creates a serious environmental concern, and an explosion hazard if the fines are flammable. Hence, agglomerated products must be capable of resisting attrition during the handling and processing stages.

The importance of the attrition of catalysts is recognized in the catalysis community. ASTM has developed standards for quantifying the attrition of catalysts and catalyst carriers using cylindrical drums, mechanical sieve shaker, or air jets (11-13). Particle shapes for which the attrition test applies include tablets, extrudates, spheres, and irregularly shaped particles. Particle sizes occur in the range of 2-19 mm for the drums, and 10-180 μm for the air jets. However, these tests are not quite applicable to the Fe-catalysts being prepared for bubble column reactors since these catalysts are quite weak. Without an appropriate method to measure

attrition resistance, it is difficult to do research on improving the attrition resistance of these catalysts.

This study describes two approaches we have used to measure the strength or attrition resistance of a heterogeneous catalyst. These methods include uniaxial compaction and ultrasonic fragmentation. The Fe F-T catalyst was compared to a sample of catalyst support that is representative of strong agglomerates. Best-fit lines as well as a mathematical model were used to quantify the strength via uniaxial compaction method, and these results were compared to the qualitative results obtained from ultrasonic fragmentation.

## Overview of Attrition Tests

### *Uniaxial Compaction Method*

Uniaxial compaction is a method in which a sample confined in a cylindrical die is compressed uniaxially under a load. This method is an alternative to the conventional method in which individual particles are crushed between two platens (14). Individual particles show a distribution of strengths. To obtain a reliable average strength, many particles must be tested. Hence, uniaxial compaction is often used in place of the conventional method.

Glass *et al.* (15,16) at Sandia National Laboratories showed that compaction generally occurred in two stages (Figure 1). In the first regime, the gradual increase in relative density is due to particles, such as granules and agglomerates, sliding and rearranging without fracture. At this stage little compaction occurs, and only a small percentage of the void space is removed during rearrangement. It is often observed experimentally that this regime has a slope of »0.003-0.005. In the second regime, a sharp increase in relative density is due to deformation and fracture in conjunction with the sliding and rearrangement of particles (slope»0.2). At this stage a larger percentage of void space is removed during rearrangement. Beyond the second regime there may be another characteristic slope at higher pressures, but this has not been analyzed because it is still not well understood. The intersection of these slopes in the two regimes is called the breakpoint, which has been used as a semi-quantitative indicator of average strength. If all particles or agglomerates had the same strength and were in regular array, they would start to collapse at the same pressure and the breakpoint would be seen as a sharp discontinuity (17). No discontinuity, however, is observed for most materials due to large variations in strength among particles. This variability was assumed to be attributed to a variation in the flaw size as well as in the size and shape of particles. However, if best-fit lines were drawn through the data in the two linear regimes, an average strength value could be obtained.

Instead of measuring strength based on best-fit lines, average strength could be predicted via mathematical models. For example, Ciftcioglu *et al*. (18) calculated agglomerate strength curves for yttria powders using the Rumpf equation (19). This equation, however, was based on the assumption that the particles were monodispersed and spherical, and that there was instantaneous failure at all points, which contradicted the experimental observations of Glass (15). Adams *et al*. (20) derived a model which correlated pressure to natural strain to obtain an average cohesive strength on a bed of agglomerates. Other models included a theoretical model by Kenkre *et al*.

(21) capable of predicting various powder properties, and a model derived by Song *et al*. (22) to estimate agglomerate tensile strength of ceramic powders.

Glass *et al.* eliminated the effects of shape and size factors by performing uniaxial compaction tests on uniform-size glass spheres. They found that, surprisingly (15), glass spheres with uniform shape and size also exhibited very large variations in strength. One possible reason for the high variability in strength of the glass spheres was that a large range in flaw sizes may be present.

*Ultrasonic Fragmentation Method*

Thoma *et al.* (23) at the University of New Mexico developed a characterization technique to quantitatively determine agglomerate strength distributions by exposing a powder dispersion to a calibrated ultrasonic field and following the changes via particle size analysis. The ultrasonic disrupter in the calibration study was a 20kHz Tekmar TSD-500 Sonic Disrupter equipped with a V1A horn having a 1/2" tip. The ultrasonic forces were calibrated at various energy level settings for a fixed amount of time via an ultrasonic disrupter using various types of hollow glass bubbles. The bubbles that could not be broken via ultrasound were then crushed in a mercury porosimeter, and hence the effective pressure during ultrasonic excitation could be calibrated. Table 1 gives power output and breakage pressures for a given control setting (24). Determination of the effective breaking pressures involved ascertaining the pressure at which the untreated glass bubble strength distributions merged. Weaker bubbles were used for settings lower than 5, and stronger bubbles were used for settings 5 and above.

*Fragmentation Mechanism*

Ultrasonic fragmentation of agglomerates (i.e., size reduction) is caused by interaction of cavitation bubbles with adjacent agglomerated particles. Such cavitation causes breakage via the expansion and subsequent violent collapse of these bubbles, creating intense pressures in the vicinity of the collapse (25), which is the primary means of agglomerate comminution (Figure 2).

Two mechanism for particle breakdown have been determined: erosion and fracture. Erosion is a process where primary particles are dislodged from the surface of the agglomerate when the cavitation pressure exceeds the agglomerate strength. Kusters *et al.* reported that the amount of erosion is proportional to the geometric surface area (i.e., external surface) of the parent agglomerate. Fracture is the division of the original agglomerate into several smaller agglomerates, and results from crack propagation through the agglomerate compact. Stresses exerted on the agglomerate cause the initiation and propagation of surface flaws. When the cavitation pressure is below the agglomerate strength of a given powder, then a time lag is observed where crack propagation occurs, weakening the compact, until fragmentation proceeds unhindered. The time lag to unhindered fragmentation will decrease with increasing cavitation stress, and is directly related to agglomerate strength since the time lag will become negligibly small as the cavitation pressure becomes equal to the agglomerate strength. In analogy to mechanical fracture testing (i.e., the Charpy test), the fracture toughness of an agglomerate

powder could be defined by the energy required to achieve a certain amount of product fines given the cavitation pressure is equal to the agglomerate strength. The relative fracture toughness could also be used as a measure of relative agglomerate strength. Such a postulate might be confirmed by using comparing agglomerate fracture by ultrasonication of powders of known strengths by tensile testing methods, e.g., the method of Rumpf, Pietsch *et al.*, and Schubert *et al.* (26-28).

## Experimental

*Ultrasonic Fragmentation*

A 0.5% sodium hexametaphosphate (SHMP; Aldrich Chemicals) solution was prepared by mixing 0.5 g of SHMP with 1 L of deionized water. VISTA-B-965-500C (alumina support) was used as a test sample, representing strong agglomerates, and compared to a UCI-LAPI-COMP-DRUMC catalyst (47.63% Fe, 3.75% Cu, 3.74% K, 5.28% Si by weight), a catalyst used previously in DOE pilot plant tests.

In a typical run, 1 g of catalyst sample was added to 50 ml of the 0.5% SHMP solution which was used as a dispersant. A Micromeritics Sedigraph 5100 analyzer was used to measure the particle size distribution at time 0 min. The suspension was then subjected to ultrasonic energy at an amplitude setting of 20 at 5 min intervals using a Tekmar 501 ultrasonic disrupter equipped with a V1A horn and a 1/2" probe tip (a setting of 20 is equivalent to a setting of 2 for the Tekmar 500 ultrasonic disrupter). After different extents of ultrasonic irradiation, the particle size distribution was analyzed to detect the mode of particle fragmentation.

*Uniaxial Compaction*

The VISTA alumina support was used for the uniaxial compaction tests. In a typical run, 10 mg were loaded into the cell of a die with a 1/8" opening. A plunger was then placed on top of the filled die, taking great care not to compress the sample. To account for the error due to deformation of the top plunger and to the compliance of the crosshead, the displacement of the empty fixture as a function of load was subtracted from the displacement of the filled die.

Compaction tests were conducted by placing the filled die underneath the crosshead of the Instron 5565 machine. The crosshead was manually lowered such that it was just touching the top plunger. The displacement gauge was zeroed, and the crosshead was then activated at a rate of 1.00 mm/min. Testing was continued until a load of 1000 N was reached. The sample was repeated for reproducibility.

This same analysis procedure was then applied to the UCI catalyst, and compared to the VISTA alumina support.

## Results and Discussion

Figure 3 shows semilogarithmic plots of compaction curves for the VISTA-B-965-500C alumina support. The relative density was calculated using the mass of the sample, initial compact height, measured displacement, and theoretical density. No obvious breakpoints in the

compaction curves were observed due to the variability in strengths (17), but if best-fit lines were drawn through the data in the two linear regimes, an average breaking strength value could be obtained. The breaking strength was determined to be 11.97 MPa from Fig. 3a. The test shown in Fig. 3b yielded a curve that was almost identical to that of Fig. 3a, but a lower slope (not shown) at high loads yielded a breaking strength of 6 MPa. Glass *et al*. (15) suggested that as long as the aspect ratio $L_f/D$ was £ 1.2, consistent compaction results would be produced. Although the aspect ratio fit this criterion (0.61 for Fig. 3a vs. 0.74 for Fig. 3b), consistent results were not obtained due to factors such as individual particle sizes and shapes, the place at which the samples were taken from the sample in the bottle, and the disturbance of the sample in the die during placement of the top plunger.

The breaking strength via best-fit lines has been found to be sensitive to how many data points are included in determining the slope of the two linear regimes. Hence, we have explored alternative methods to derive the breaking strength. Figure 4 shows compaction data for the VISTA alumina sample. The data were presented in the form of a plot of ln(P) vs. natural strain, e, defined as $\ln(h_o/h)$ where $h_o$ is the initial height and h is the measured height. The results were analyzed using a mathematical model presented by Adams *et al.* (20) which yielded a value for the breaking strength (sigma) of the particles within the sample. Except for the data below e = 0.2, the model closely fits with the data for e above 0.2. Deviations from the model for $e < 0.2$ may be due to experimental errors based on parameters, such as particle size distribution, during the rearrangement of particles and before the onset of compaction. The breaking strengths determined from the model were 7.44 MPa for Fig. 4a and 4.89 MPa for Fig. 4b. In Figure 3, the breaking strengths differed by about a factor of 2, whereas in Figure 4, they differed by about a factor of 1.5. Although the factors between them do not differ by much, the method using a mathematical model does appear to be less sensitive to variations in the analysis procedure, as is the breakpoint data.

Figure 5 shows a cumulative mass distribution plot of mass finer (%) vs. equivalent spherical diameter for the VISTA alumina sample. According to this plot, there was little attrition after 15 min of ultrasonic irradiation, indicating that erosion was the dominant fragmentation mechanism. Figure 6 shows a cumulative mass distribution plot for the UCI catalyst. According to this plot, fracture was the dominant fragmentation mechanism, along with some generation of fine particles due to erosion. Figure 7 shows compaction data for the VISTA alumina support and the UCI F-T catalyst, fitted with the mathematical model. Figures 5 and 6 showed significant differences in strength by the ultrasonic fragmentation method, while in Figure 7 their strengths differed by about 1.2 MPa via the uniaxial compaction method. Hence, the ultrasonic fragmentation method seems to be more sensitive to the differences between these powders, that are not seen in the compaction method.

We have also explored the use of the ultrasonic fragmentation method for a Fe F-T catalyst that doe not contain any silica, and a Fe F-T catalyst containing a kaolin binder. Figure 8 shows a cumulative mass distribution plot for these catalysts. The catalyst containing the kaolin binder was very weak, comparable to the binderless catalyst. Further analysis using transmission electron microscopy (TEM; Figure 9) showed that kaolin and Fe F-T catalyst occurred as two distinct phases, and that both had plate-like structures which did not connect to create strong

interlocking forces between them. Therefore, binders with other morphologies should be explored to provide improved attrition resistance in these catalysts.

## Summary

Two methods were explored for their application in measuring the strength or attrition resistance of heterogeneous catalysts: uniaxial compaction and ultrasonic fragmentation. The VISTA alumina support was used to determine the applicability of the uniaxial compaction tests. The breaking strength determined from the breakpoint was found to be sensitive to how many data points were included in determining the slope of the two linear regimes. As an alternative method, average strength was predicted via a mathematical model. However, neither approach provided very consistent results in replicate tests from a given sample. The compaction method was also not able to reveal differences in strength among dissimilar catalysts. The Fe catalyst is considerably weaker than the alumina support, but the strength measured via compaction showed differences in strength of 1.2 MPa, well within the variation seen within a given sample. On the other hand, cumulative mass distribution plots showed significant differences in strength by ultrasonic fragmentation. Erosion was the dominant fragmentation mechanism for VISTA alumina while fracture was the dominant mechanism for the UCI catalyst, both after 15 min of ultrasonic irradiation.

The ultrasonic fragmentation method was used for a Fe F-T catalyst that contained no binder and one that contained a kaolin binder. The results indicate that a plate-like morphology in a binder is not suitable for providing improved agglomerate strength. The role of other binder morphologies on the strength of spray-dried agglomerates is being pursued in our laboratory.

## Acknowledgments

The authors would like to thank the U.S. Department of Energy and the Federal Energy Technology Center (FETC) under contract no. DE-FG22-95PC95210 for their financial support of this project. The authors also thank Robert Gormley and his associates at FETC for providing us with the catalysts and support, and for helpful discussions.

## References

1. Bukur, D. B., "Development of Precipitated Iron Fischer-Tropsch Catalysts. Quarterly Technical Progress Report", Performer: Texas A&M University, College Station, Department of Chemical Engineering, PR: PC A04/MF A01.
2. Davis, B. H., "Technology Development for Iron Fischer-Tropsch Catalysis. Quarterly Technical Progress Report", Performer: Kentucky University, Research Foundation, Lexington, PR: PC A04/MF A01.
3. Bhatt, B. L., "Liquid Phase Fischer-Tropsch (II) Demonstration in the LaPorte Alternative Fuels Development Unit", Performer: Air Products and Chemicals, Inc., Allentown, PA, PR: PC A07/MF A02.
4. Saxena, S.C., *Catalysis Rev. Sci. Engr.*, *37* (1995) 227.

5. Parkinson, G., *Chem. Engr.* (1997) 39.
6. Raje, A., Inga, J.R., and Davis, B.H., *Fuel*, *76* (1997) 273.
7. Stern, D., Bell, A.T., and Heinemann, H., *Ind. Eng. Chem. Des. Dev.*, *24* (1985) 1213.
8. Bukur, D.B., Nowicki, L., and Patel, S.A., *Canadian J. Chem. Engr.*, *74* (1996) 399.
9. Dynys, F.W. and Halloran, J.W., *J. Am. Ceram. Soc.*, *64* (1981) 596.
10. Lange, F.F. and Metcalf, M., *J. Am. Ceram. Soc.*, *66* (1983) 398.
11. 1996 Annual Book of ASTM Standards, Vol. 05.03, Designation: D4058-92, 979.
12. 1996 Annual Book of ASTM Standards, Vol. 04.02, Designation: C136-95a, 78.
13. 1996 Annual Book of ASTM Standards, Vol. 05.03, Designation: D5757-95, 1064.
14. Bemrose, C.R. and Bridgwater, J., *Powder Tech.*, *49* (1987) 97.
15. Glass, S.J., Ewsuk, K.G., and Readey, M.J., SAMPE Technology Conference, Albuquerque, NM, 1995.
16. Glass, S.J. and Newton, C., ACERS Symposium on Science, Technology, and Commercialization of Powder Synthesis and Shape Forming Processes, Cincinnati, OH, 1995.
17. Ciftcioglu, M., Akinc, M., and Burkhart, L., *Am. Ceram. Soc. Bull.*, *65* (1986) 1591.
18. Ciftcioglu, M., Akinc, M., and Burkhart, L., *Am. Ceram. Soc. Bull.*, *65* (1986) 1591.
19. Rumpf, H., Agglomeration, K.V. Sastry, New York, 1977.
20. Adams, M.J., Mullier, M.A., and Seville, J.P.K., *Powder Tech.*, *78* (1994) 5.
21. Kenkre, V.M., Endicott, M.R., Glass, S.J., and Hurd, A.J., *J. Am. Ceram. Soc.*, *7 9* (1996) 3045.
22. Song, J-H and Evans, J.R.G., *J. Am. Ceram. Soc.*, *77* (1994) 806.
23. Thoma, S.G., Ciftcioglu, M., and Smith, D.M., *Powder Tech.*, *68* (1991) 53.
24. Thoma, S.G., Ciftcioglu, M., and Smith, D.M., *Powder Tech.*, *68* (1991) 71.
25. Webster, E., *Ultrasonics*, Jan-Mar (1963) 39.
26. Rumpf, H., Agglomeration, Knepper, W.A., (Ed.), New York: Wiley Interscience, 1962.
27. Pietshch, W.B., Hoffman, E., and Rumpf, H., *Ind. Engr. Chem. Prod. Res. Ed.*, *8* (1969) 58.
28. Schubert, H., Herrmann, W., and Rumpf, H., *Powder Tech.*, *11* (1975) 121.

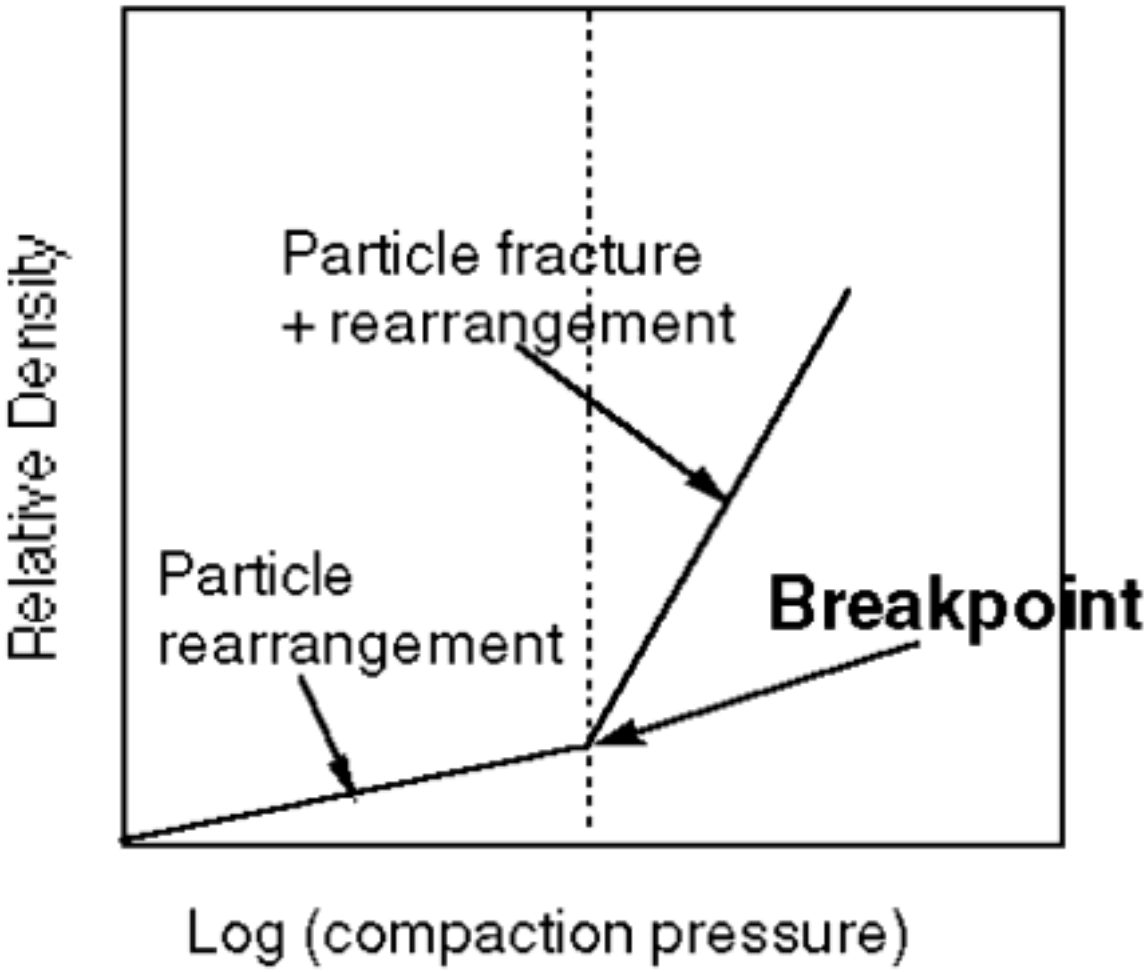


Figure 1 Semilogarithmic compaction curve. Compaction generally occurs in two stages: granule rearrangement and sliding without fracture, and local deformation and fracture with granule rearrangement

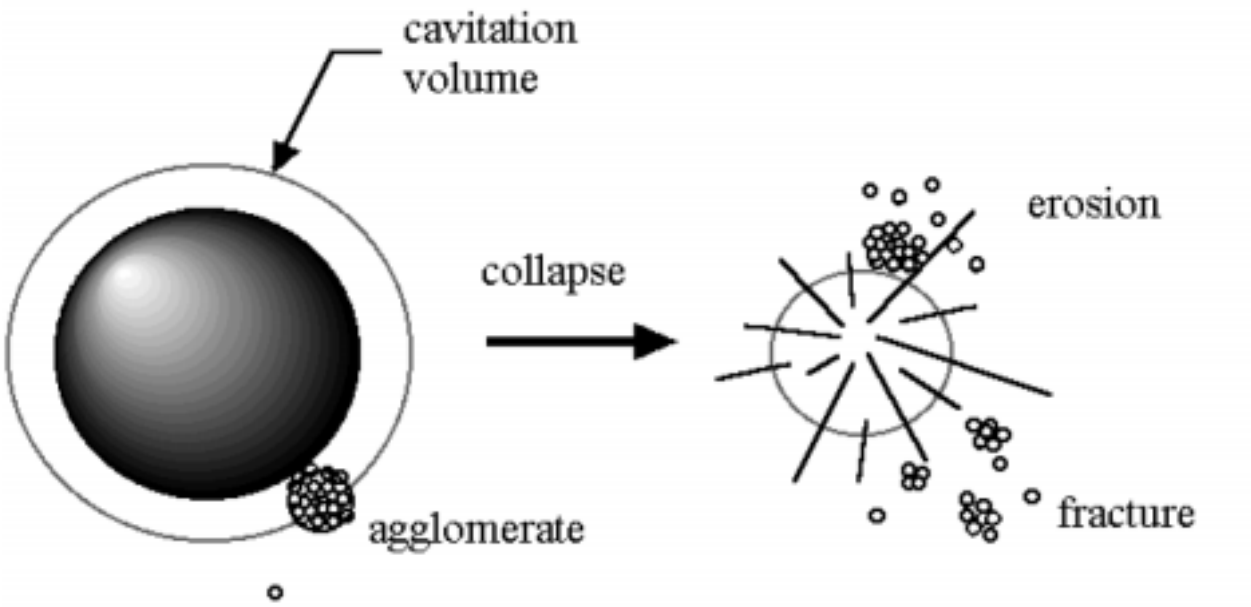


Figure 2 Schematic of the cavitation mechanism for agglomerate comminution. The two mechanisms, erosion and fracture, are illustrated.

Fig. 3a

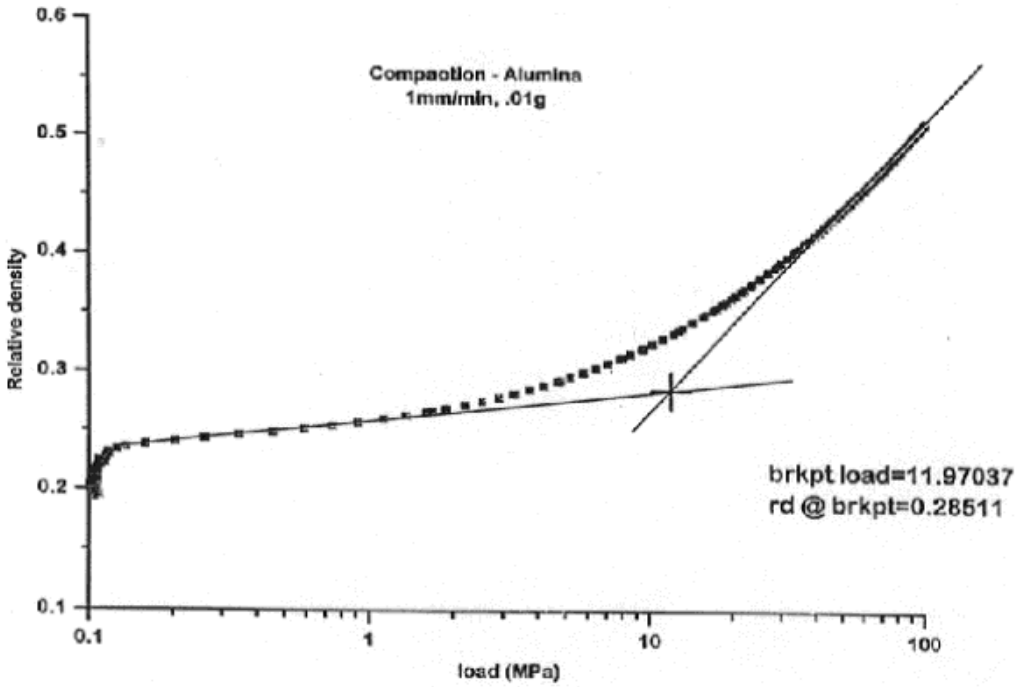


Fig. 3b

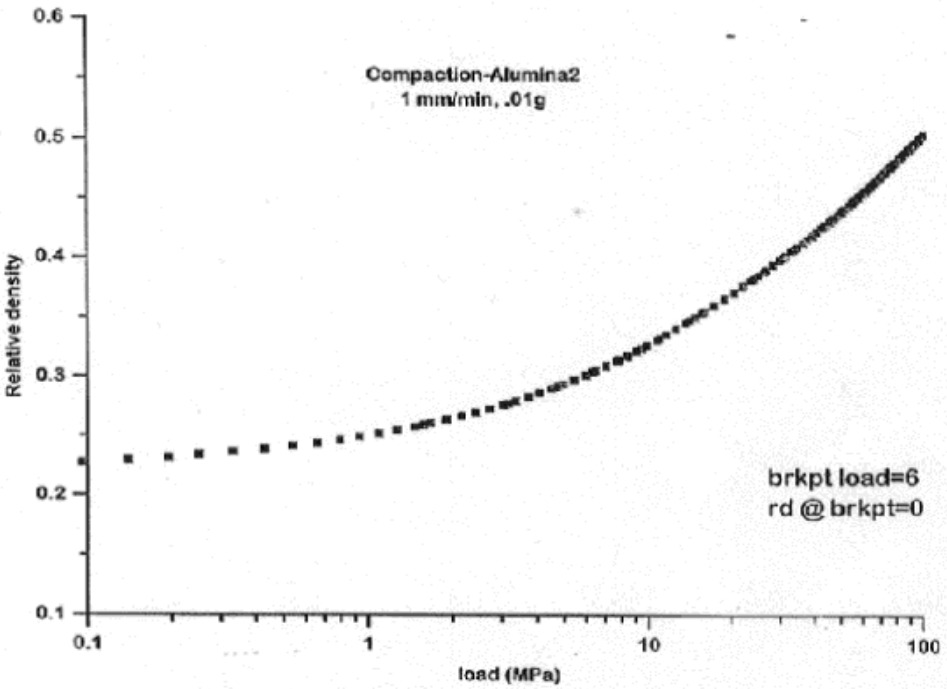


Figure 3. Semilogarithmic plots for the VISTA-B-965-500C alumina support. For Fig. 3a, the relative density vs. log P curve can be fit by two linear segments whose intersection determines a nominal breaking strength (11.97 MPa). For Fig. 3b, the compaction curve up to a pressure of 30 MPa is very similar to that of Fig. 3a. However, using linear fits to the data yields a nominal breaking strength of 6 Mpa.

Fig. 4a

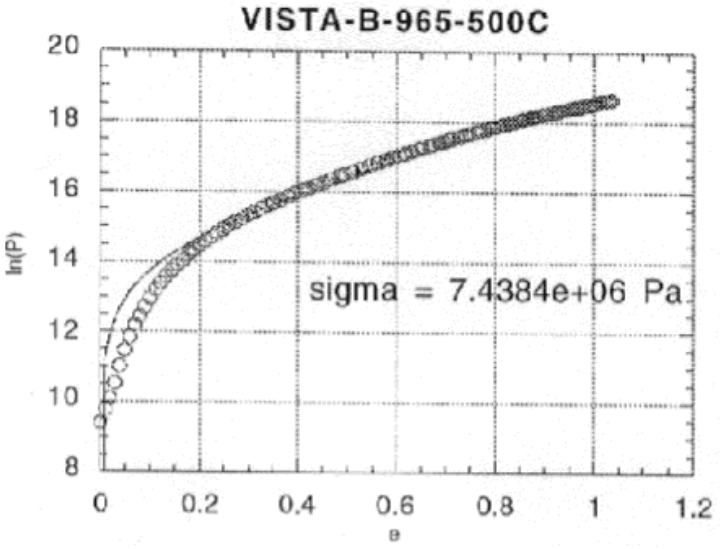


Fig. 4b

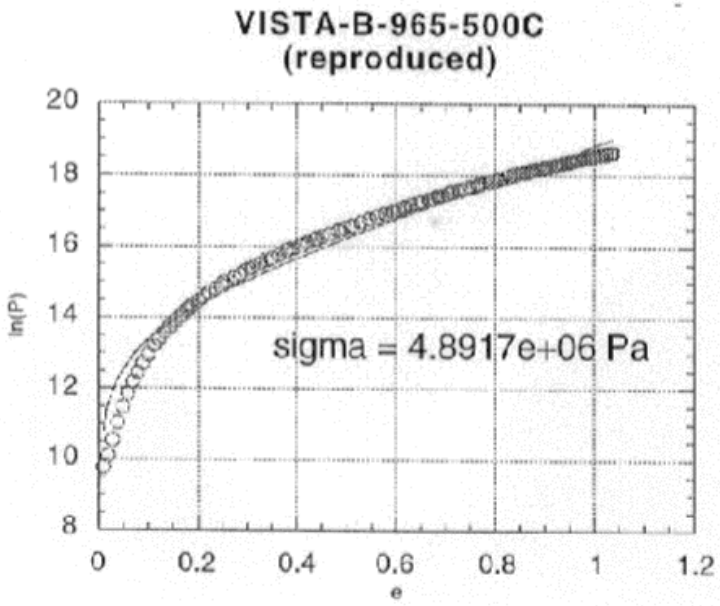


Figure 4. Compaction data for the VISTA alumina support. A mathematical model presented by Adams *et al.* (20) yields a value for the breaking strength (sigma) of the particles within the sample. The model closely fits the data, and the strengths are determined to be 7.4 MPa for Fig. 4a and 4.9MPa for Fig. 4b.

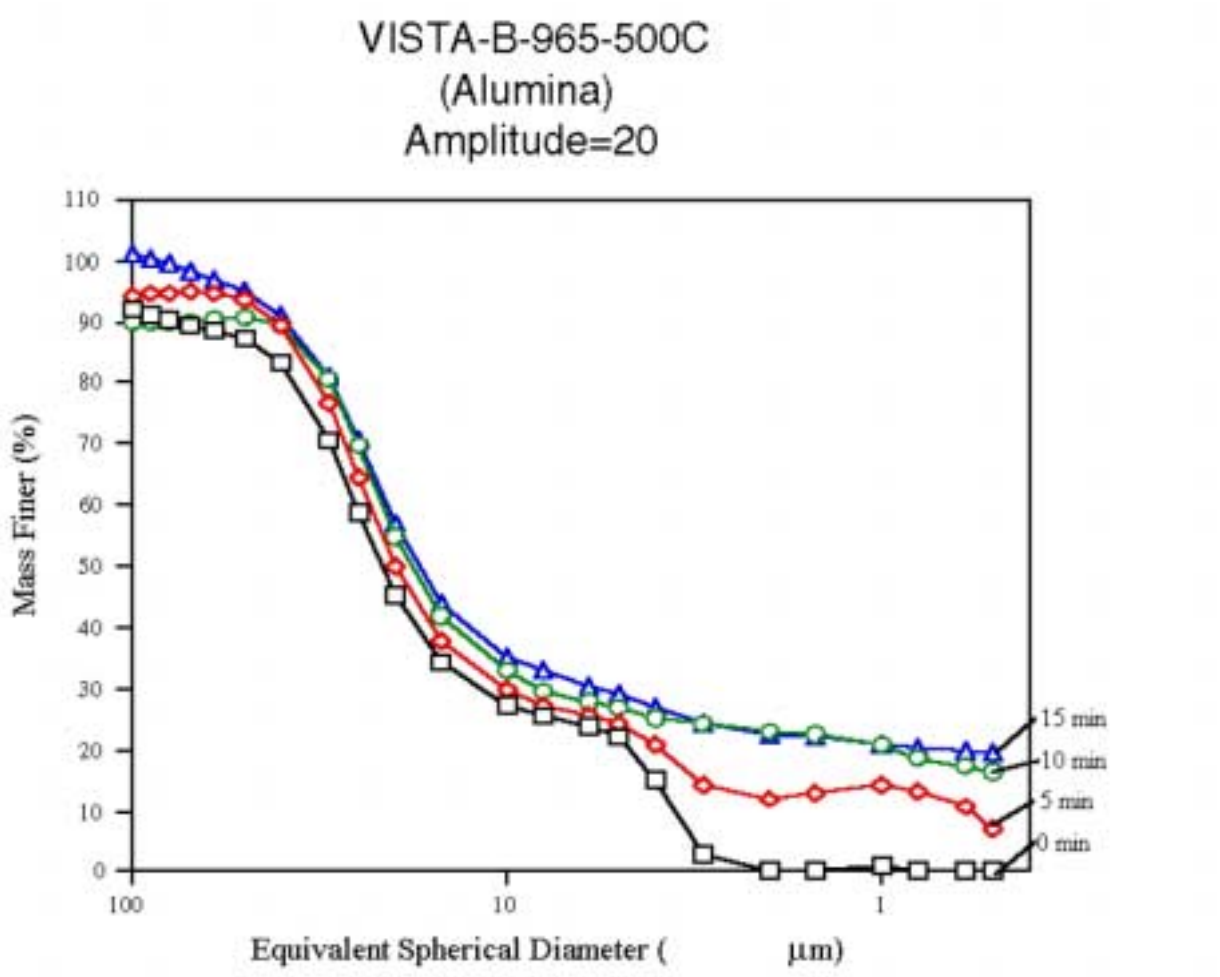


Figure 5 Sedigraph particle size distribution of VISTA-B-965-500C sample. The starting alumina from VISTA was sieved and calcined in air at 500°C. Very little fragmentation occurs after 15 min of ultrasonic irradiation, although some erosion has occurred.

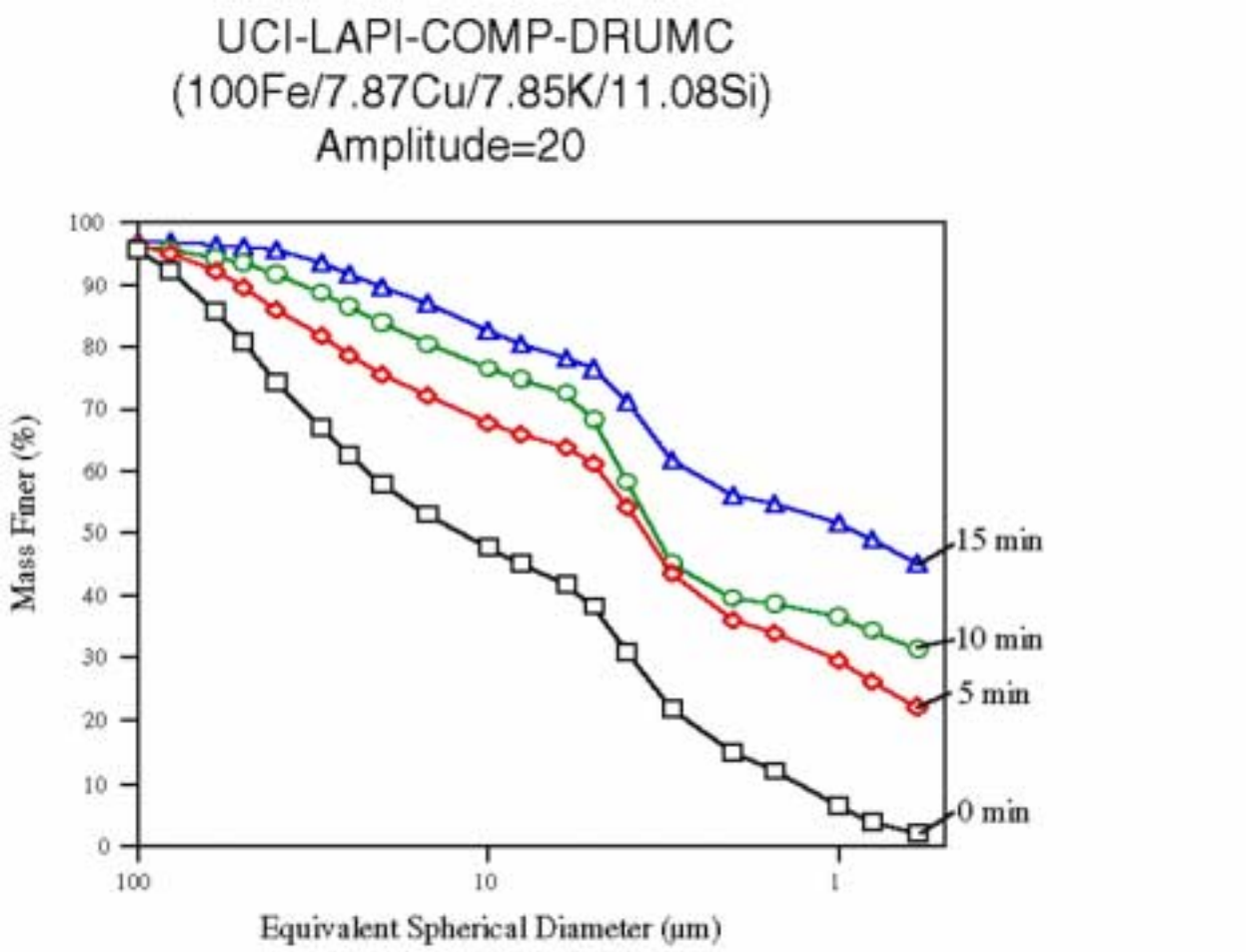


Figure 6 Sedigraph particle size distribution for UCI F-T catalyst UCI-LAPI-COMP-DRUMC, used previously in DOE pilot plant tests. There is considerable particle breakdown and generation of fine particles after 15 min of ultrasonic irradiation.

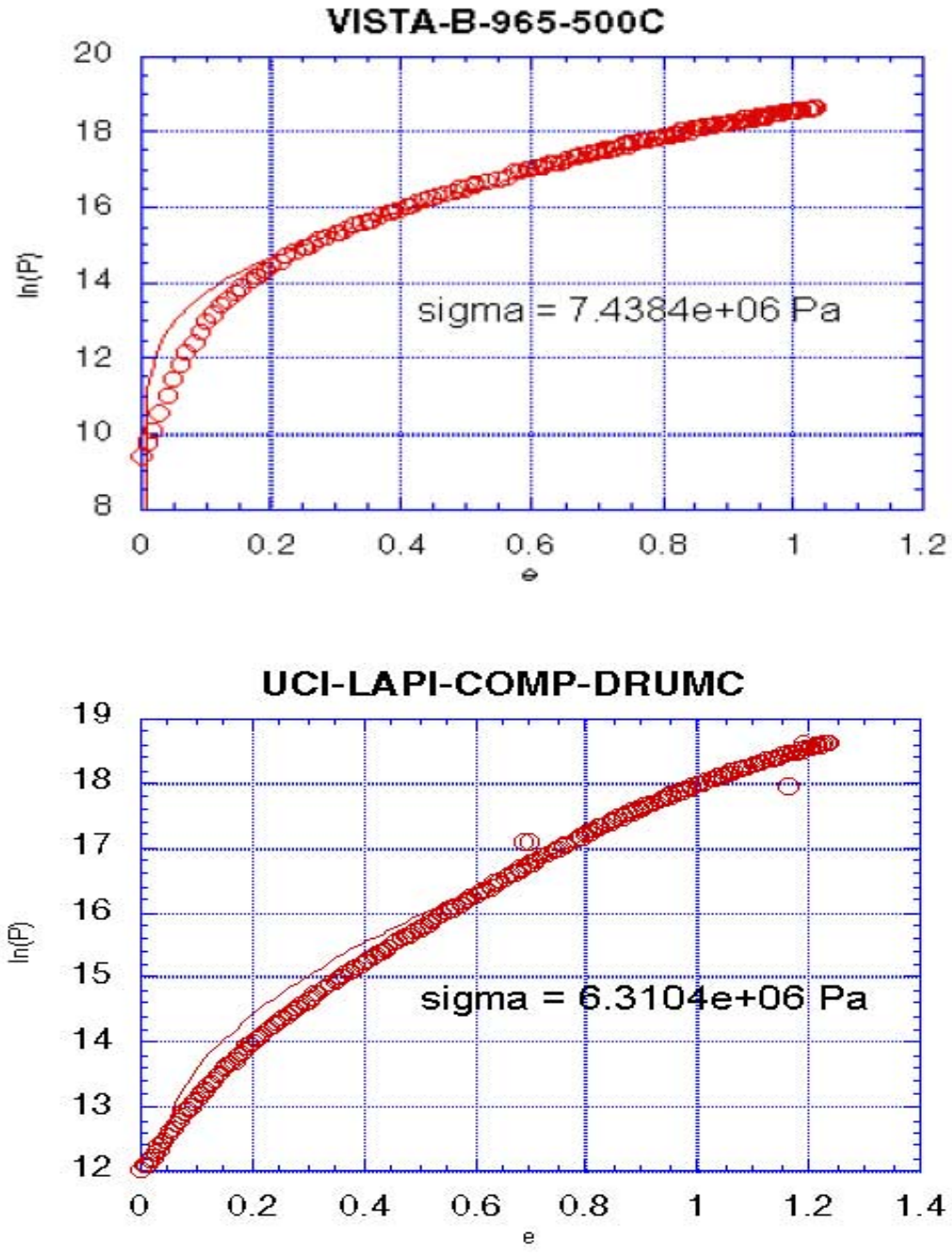


Figure 7 Compaction data for the VISTA alumina support and the UCI F-T catalyst. A mathematical model presented by Adams *et al*. (20) yields a value for the breaking strength (sigma) of the particles within the sample. The strength for the UCI catalyst is determined to be 6.3 MPa, and the strengths between these samples differ by about 1.2 MPa.

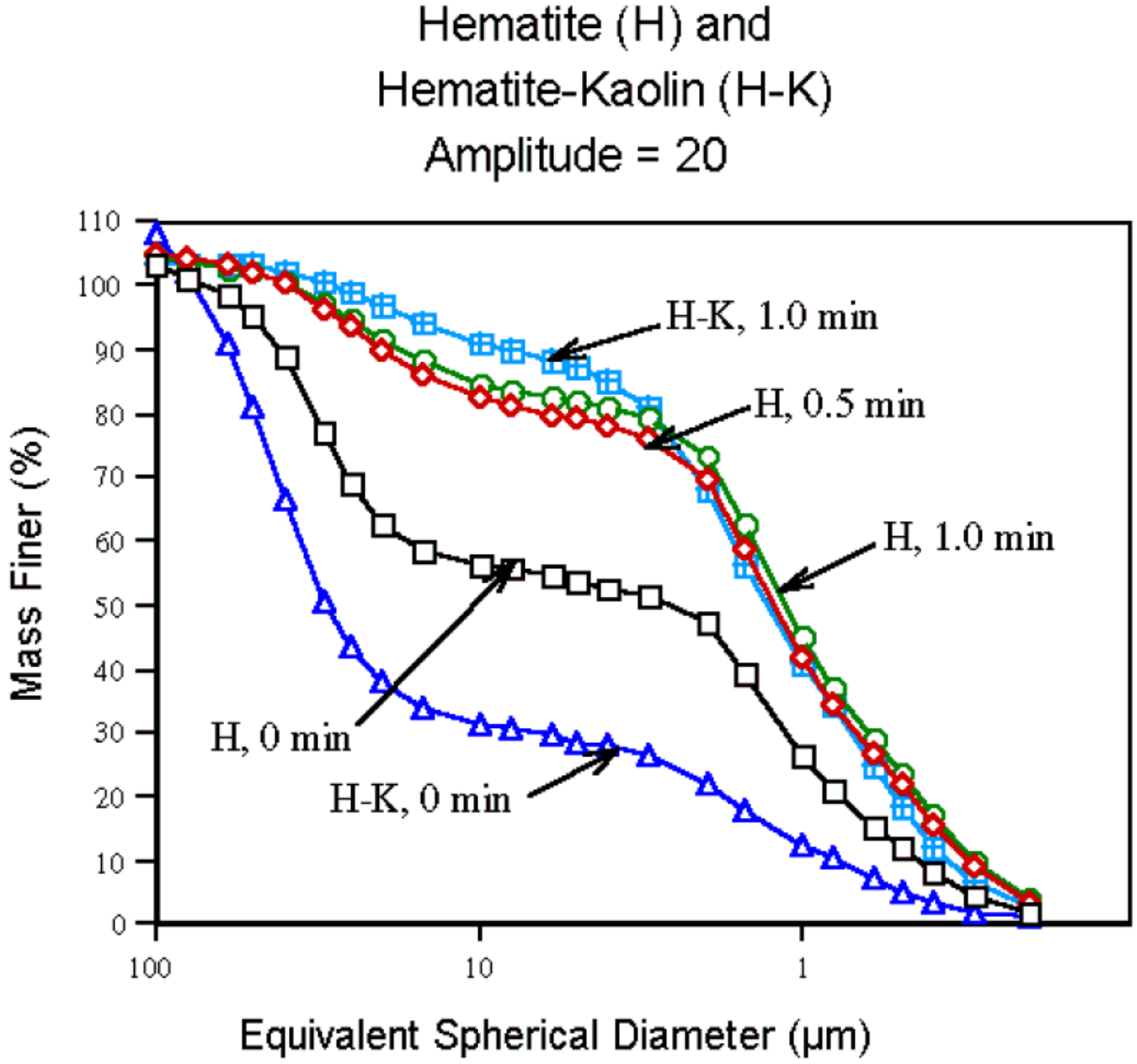


Figure 8 Comparison of the breakdown of the binderless catalyst with the kaolin binder containing Fe F-T catalysts. The kaolin binder does not impart any additional strength to the catalyst.

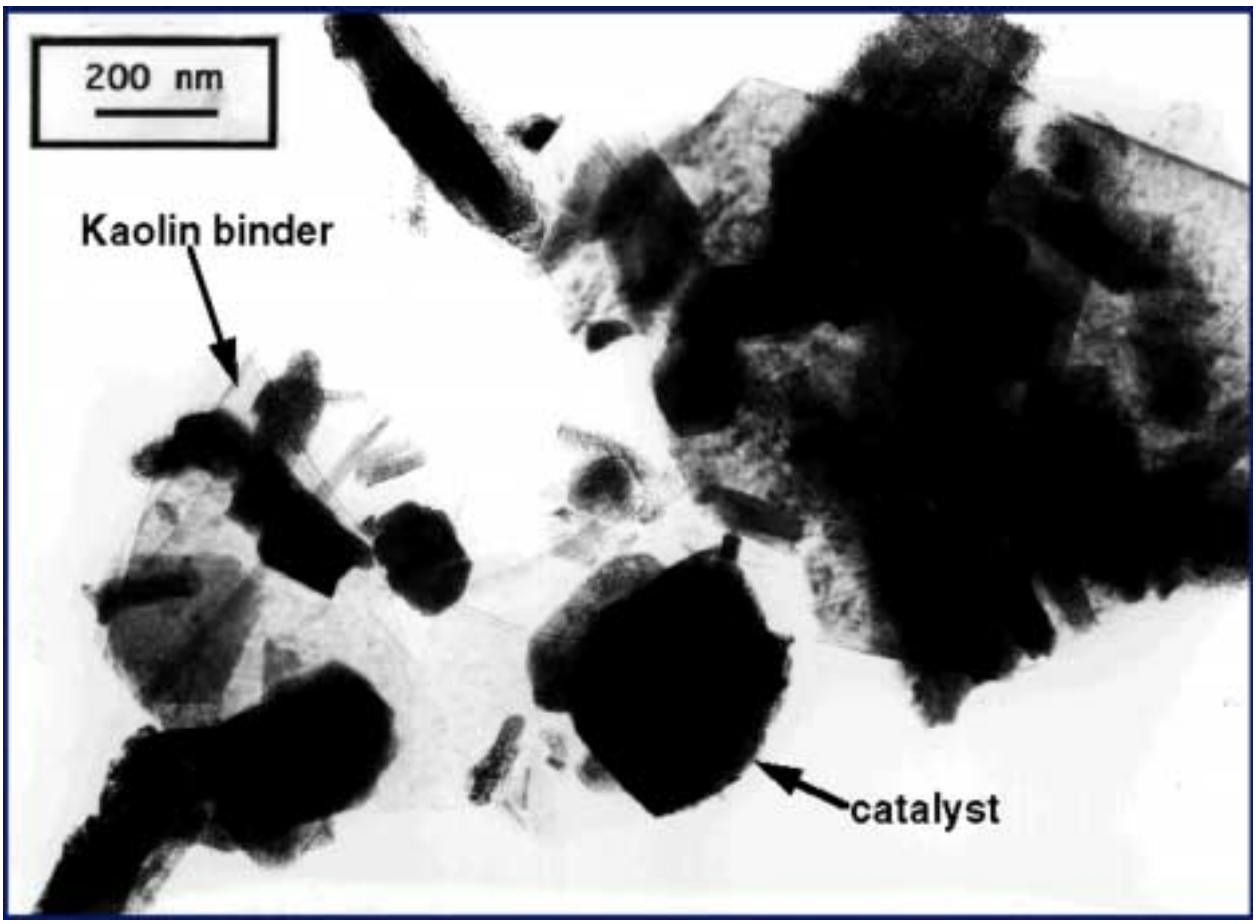


Figure 9 TEM picture of a commercial Fe catalyst with a kaolin binder. Kaolin and Fe catalyst occurs as two distinct phases, and that both have plate-like structures which do not connect to create strong interlocking forces between them.

**Table 1.** Ultrasonic power output, ε, and breaking stress, σ, for a given control setting, N.

| Setting, N | Power (W) | Stress ($lbs/in^2$) | Setting, N | Power (W) | Stress ($lbs/in^2$) |
|---|---|---|---|---|---|
| 1.0 | 1.06 | 150 | 6.0 | 19.25 | 5,150 |
| 2.0 | 2.13 | 200 | 7.0 | 29.57 | 6,000 |
| 3.0 | 3.19 | 350 | 8.0 | 55.32 | 9,950 |
| 4.0 | 5.32 | 1,250 | 9.0 | 79.79 | 10,200 |
| 5.0 | 13.2 | 4,350 | 10.0 | 100.85 | 11,500 |

Thoma, S.G., Ciftcioglu, M., and Smith, D.M., *Powder Tech.*, *68* (1991) 53.